

# Fabrication of high-aspect-ratio grooves in silicon using femtosecond laser irradiation and oxygen-dependent acid etching

An Pan, Jinhai Si, Tao Chen,\* Yuncan Ma, Feng Chen, and Xun Hou

Key Laboratory for Physical Electronics and Devices of the Ministry of Education & Shaanxi Key Lab of Information Photonic Technique, School of Electronics & Information Engineering Xi'an Jiaotong University, No. 28, Xianning West Road, Xi'an, 710049, China

\*tchen@mail.xjtu.edu.cn

**Abstract:** We demonstrated a new method to fabricate micron-sized grooves with high aspect ratios in silicon wafers by combining femtosecond laser irradiation and oxygen-dependent acid etching. Femtosecond laser was employed to induce structure changes and incorporate oxygen into silicon, and then materials in oxygen-containing regions were etched by hydrofluoric acid (HF) solution to form grooves. The etching could be attributed to the reaction between HF and silicon oxides formed by femtosecond laser irradiation. The dependences of the aspect ratios of grooves on the laser fluence and the scanning velocity were also investigated.

©2013 Optical Society of America

**OCIS codes:** (320.2250) Femtosecond phenomena; (230.4000) Microstructure fabrication; (350.3850) Materials processing; (160.6000) Semiconductor materials.

---

## References and links

1. M. Shen, J. E. Carey, C. H. Crouch, M. Kandyla, H. A. Stone, and E. Mazur, "High-density regular arrays of nanometer-scale rods formed on silicon surfaces via femtosecond laser irradiation in water," *Nano Lett.* **8**(7), 2087–2091 (2008).
2. G. Miyaji, K. Miyazaki, K. Zhang, T. Yoshifuji, and J. Fujita, "Mechanism of femtosecond-laser-induced periodic nanostructure formation on crystalline silicon surface immersed in water," *Opt. Express* **20**(14), 14848–14856 (2012).
3. T. H. Her, R. J. Finlay, C. Wu, S. Deliwala, and E. Mazur, "Microstructuring of silicon with femtosecond laser pulses," *Appl. Phys. Lett.* **73**(12), 1673–1675 (1998).
4. H. Föll, M. Christophersen, J. Carstensen, and G. Hasse, "Formation and application of porous silicon," *Mater. Sci. Eng. Rep.* **39**(4), 93–141 (2002).
5. K. Juodkazis, J. Juodkazytė, P. Kalinauskas, T. Gertus, E. Jelmakas, H. Misawa, and S. Juodkazis, "Influence of laser microfabrication on silicon electrochemical behavior in HF solution," *J. Solid State Electrochem.* **14**(5), 797–802 (2010).
6. T. H. R. Crawford, A. Borowiec, and H. K. Haugen, "Femtosecond laser micromachining of grooves in silicon with 800 nm pulses," *Appl. Phys., A Mater. Sci. Process.* **80**(8), 1717–1724 (2005).
7. A. Kiani, K. Venkatakrishnan, B. Tan, and V. Venkataramanan, "Maskless lithography using silicon oxide etch-stop layer induced by megahertz repetition femtosecond laser pulses," *Opt. Express* **19**(11), 10834–10842 (2011).
8. T. Chen, J. Si, X. Hou, S. Kanehira, K. Miura, and K. Hirao, "Photoinduced microchannels inside silicon by femtosecond pulses," *Appl. Phys. Lett.* **93**(5), 051112 (2008).
9. K. Grigoras, A. J. Niskanen, and S. Franssila, "Plasma etched initial pits for electrochemically etched macroporous silicon structures," *J. Micromech. Microeng.* **11**(4), 371–375 (2001).
10. P. Mukherjee, T. H. Zurbuchen, and L. J. Guo, "Fabrication and testing of freestanding Si nanogratings for UV filtration on space-based particle sensors," *Nanotechnology* **20**(32), 325301 (2009).
11. N. Gadegaard, E. Martinez, M. O. Riehle, K. Seunarine, and C. D. W. Wilkinson, "Applications of nano-patterning to tissue engineering," *Microelectron. Eng.* **83**(4-9), 1577–1581 (2006).
12. W. Noell, P.-A. Clerc, L. Dellmann, B. Guldemann, H. P. Herzig, O. Manzardo, C. R. Marxer, K. J. Weible, R. Dändliker, and N. de Rooij, "Applications of SOI-based optical MEMS," *IEEE J. Sel. Top. Quantum Electron.* **8**(1), 148–154 (2002).
13. W. Ong, J. Kee, A. Ajay, N. Ranganathan, K. Tang, and L. Yobas, "Buried microfluidic channel for integrated

- patch-clamping assay,” *Appl. Phys. Lett.* **89**(9), 093902 (2006).
14. R. Hintsche, Ch. Kruse, A. Uhlig, M. Paeschke, T. Lisec, U. Schnakenberg, and B. Wagner, “Chemical microsensor systems for medical applications in catheters,” *Sens. Actuators B Chem.* **27**(1-3), 471–473 (1995).
  15. M. Kuttge, H. Kurz, J. G. Rivas, J. A. Sánchez-Gil, and P. H. Bolivar, “Analysis of the propagation of terahertz surface plasmon polaritons on semiconductor groove gratings,” *J. Appl. Phys.* **101**(2), 023707 (2007).
  16. E. Hendry, F. J. Garcia-Vidal, L. Martin-Moreno, J. G. Rivas, M. Bonn, A. P. Hibbins, and M. J. Lockyear, “Optical control over surface-plasmon-polariton-assisted THz transmission through a slit aperture,” *Phys. Rev. Lett.* **100**(12), 123901 (2008).
  17. E. Sarajlic, M. J. de Boer, H. V. Jansen, N. Arnal, M. Puech, G. Krijnen, and M. Elwenspoek, “Advanced plasma processing combined with trench isolation technology for fabrication and fast prototyping of high aspect ratio MEMS in standard silicon wafers,” *J. Micromech. Microeng.* **14**(9), S70–S75 (2004).
  18. P. Dong, W. Qian, H. Liang, R. Shafiqi, N. N. Feng, D. Feng, X. Zheng, A. V. Krishnamoorthy, and M. Asghari, “Low power and compact reconfigurable multiplexing devices based on silicon microring resonators,” *Opt. Express* **18**(10), 9852–9858 (2010).
  19. Q. Zhang, H. Lin, B. Jia, L. Xu, and M. Gu, “Nanogratings and nanoholes fabricated by direct femtosecond laser writing in chalcogenide glasses,” *Opt. Express* **18**(7), 6885–6890 (2010).
  20. K. Kumar, K. K. C. Lee, P. R. Herman, J. Nogami, and N. P. Kherani, “Femtosecond laser direct hard mask writing for selective facile micron-scale inverted-pyramid patterning of silicon,” *Appl. Phys. Lett.* **101**(22), 222106 (2012).
  21. Y. Ma, H. Shi, J. Si, T. Chen, F. Yan, F. Chen, and X. Hou, “Photoinduced microchannels and element change inside silicon by femtosecond laser pulses,” *Opt. Commun.* **285**(2), 140–142 (2012).
  22. J. Bonse, S. Baudach, J. Krüger, W. Kauteck, and M. Lenzner, “Femtosecond laser ablation of silicon—modification thresholds and morphology,” *Appl. Phys., A Mater. Sci. Process.* **74**(1), 19–25 (2002).
  23. A. Brodeur and S. L. Chin, “Ultrafast write-light continuum generation and self-focusing in transparent condensed media,” *J. Opt. Soc. Am. B* **16**(4), 637–650 (1999).
  24. T. Kudrius, G. Slekyas, and S. Juodkazis, “Surface-texturing of sapphire by femtosecond laser pulses for photonic applications,” *J. Phys. D Appl. Phys.* **43**(14), 145501 (2010).
  25. T. H. R. Crawford, J. Yamanaka, G. A. Botton, and H. K. Haugen, “High-resolution observations of an amorphous layer and subsurface damage formed by femtosecond laser irradiation of silicon,” *J. Appl. Phys.* **103**(5), 053104 (2008).
  26. H. Ubara, T. Imura, and A. Hiraki, “Formation of Si-H bonds on the surface of microcrystalline silicon covered with SiO<sub>x</sub> by HF treatment,” *Solid State Commun.* **50**(7), 673–675 (1984).
- 

## 1. Introduction

Microstructures, such as periodic ripples [1,2], spike structures [3], porous structures [4,5], grooves [6,7] and microchannels [8], have been well produced on silicon wafers. To fabricate these microstructures, lithography of extreme ultraviolet lithography (EUV), particle beam lithography and nano-imprint lithography have been widely applied [9–11]. Among these microstructures, high-aspect-ratio grooves have promising applications in fabrication of micro-electro-mechanical systems (MEMS), multilayer microfluidic devices and microsensors [12–14]. In addition, the fabrication of grooves also has important applications in the trench isolation CMOS technology and optical control over surface plasmon polariton assisted THz transmission [15–18].

Much research work has been conducted on the fabrication of grooves in silicon wafers. Freestanding gratings with a period of 240 nm and a depth of 1800 nm have been fabricated via a combined system including deep UV lithography and reactive-ion etching on preprocessed specimen [10]. Traditional lithography is relatively mature and can reach a max precision of nanometers magnitude.

In recent years, as a powerful way for the fabrication of microstructures, femtosecond laser direct writing has been employed extensively to machine nearly all kinds of materials, such as glasses, photo-polymers and silicon [19,20]. Up to now, the fabrication of the all-silicon grooves using femtosecond laser direct writing is mainly based on the laser ablation technique. During the process, however, the debris and resolidified molten silicon might block the energy delivery deeper into the silicon [6]. Hence, the aspect ratio of the grooves cannot be high enough. Recently, we found femtosecond laser could induce structure changes deep into silicon. In addition, the element of oxygen was incorporated into laser-induced structure change (LISC) regions [21]. If materials in LISC regions are removed selectively, grooves with high aspect ratios could be obtained without the ablating problem mentioned above.

In this paper we introduce a new method for the fabrication of micron-sized grooves with high aspect ratios in silicon wafers by combining femtosecond laser irradiation and a targeted acid etching process. Femtosecond laser at 800 nm was employed to induce LISC in silicon, and then materials in LISC regions were etched by hydrofluoric acid (HF) solution to form grooves. The etching process could be attributed to the chemical reaction between HF and silicon oxides ( $\text{SiO}_x$ ), which led to the remove of the materials in LISC regions. Meanwhile the HF solution had almost no effect on pure silicon. Grooves with an aspect ratio of 16 were fabricated in our study. What's more, we fabricated grooves at different experimental conditions to investigate influences of laser irradiation power and scanning velocity on the aspect ratios. Experimental results showed the aspect ratios of acid-etched grooves increased with the increase of the incident laser fluence and decreased with the increase of scanning velocity.

## 2. Experimental setup

There were two steps to fabricate grooves in silicon wafers, including femtosecond laser irradiating and HF etching. Details of these two steps are showed in Fig. 1.

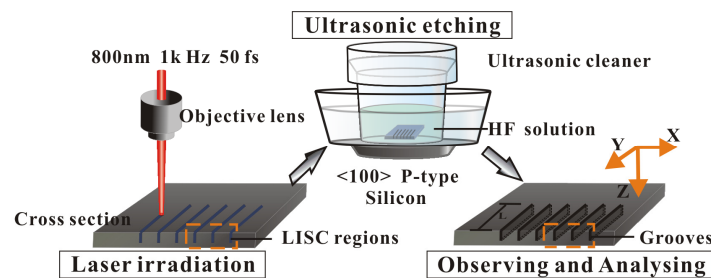


Fig. 1. Two-step schematic diagram of micron-sized grooves fabrication.

### 2.1 LISC induced by femtosecond laser irradiation

LISC was induced in the silicon wafer with a thickness of 500  $\mu\text{m}$ . The wafer was P-type with  $\langle 100 \rangle$  crystal orientation. As the first step, the wafer was fixed on a three-dimensional translation stage controlled by a computer and irradiated by femtosecond laser under ambient air conditions. The precision of the stage was 40 nm in x, y and z direction, respectively. Laser pulses were provided by a regeneratively amplified Ti:sapphire laser system. This laser system can generate 4 mJ, 50 fs laser pulses at a repetition rate of 1 kHz. The operating center wavelength is 800 nm. As showed in Fig. 1, the femtosecond laser beam was focused by a  $10 \times$  microscope objective lens (N.A. = 0.30) onto the upper surface of the silicon. LISC regions were formed by scanning the focused laser beam over silicon surfaces. The scanning direction was negative along the y axis, which was parallel to the polarization of laser pulses. The scan length was 600  $\mu\text{m}$  for each scanning line, and the separation distance was set at 80  $\mu\text{m}$  to avoid the interference between two adjacent scanning lines. A CCD camera was fixed on the microscope system to monitor the fabrication processes. The laser energy could be continuously adjusted by the variable optical attenuator in front of the microscope system.

### 2.2 Fabrication of grooves by HF etching

After femtosecond laser irradiation, HF etching was applied. Before etching, in order to remove the debris on the silicon surface, the specimen was ultrasonically cleaned by acetone alcohol and deionized water for 15 min respectively. The cleaning process had no influence on the LISC and the silicon. After cleaning the cross section of the specimen was observed using a scanning electron microscopy (SEM) and the chemical composition was analyzed by energy dispersive X-ray spectroscopy (EDX) analyzing. Then the specimen was put into a 20 wt% HF

solution for 45 min, assisted by ultrasonic cleaner at room temperature. Finally the cross section of grooves was characterized by SEM and EDX.

### 3. Experimental results and discussion

#### 3.1 Morphology features of the LISC regions and the grooves

Figures 2(a) and 2(b) illustrate the cross-sectional SEM images of the LISC regions induced at the laser fluence of  $11.14 \text{ J/cm}^2$ , which is more than the ablation threshold of silicon ( $0.2 \text{ J/cm}^2$ ) [22]. LISC regions with the length of  $104 \mu\text{m}$  were formed in silicon, which were always accompanied by surface ablation. The cross-sectional shape of the LISC region was neither convergent nor divergent, and the length was more than the Rayleigh length (about  $30 \mu\text{m}$ ) of the focused laser beam. It is possible that self-trapped filament occurred in the region. To form such  $104\text{-}\mu\text{m}$  long LISC region, the average incident power excluding reflection was about  $400 \text{ MW}$ , which was much more than the critical power of self-trapping in fused silica as  $4.3 \text{ MW}$  [23]. This was due to the much higher linear absorption of silicon at  $800 \text{ nm}$ . And the length of the LISC region was dependent on the linear absorption of silicon and the incident power. The transmittance of the  $100 \mu\text{m}$  thick silicon at  $800\text{nm}$  was measured to be about  $3.7\%$  and the fluence at this depth was about  $0.42 \text{ J/cm}^2$  corresponding to the incident laser fluence of  $11.14 \text{ J/cm}^2$ .

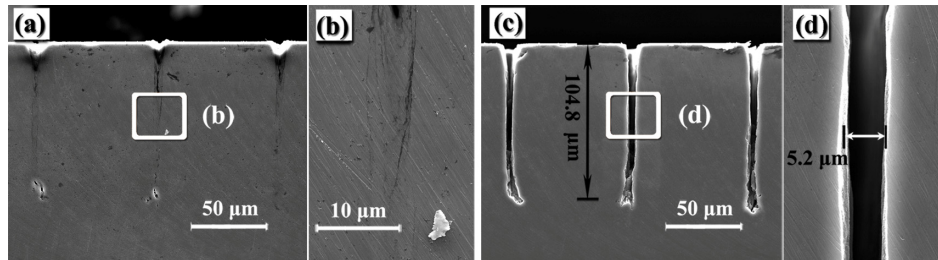


Fig. 2. Cross-sectional SEM images of LISC regions (a) before and (c) after chemical etching. (b) and (d) were the detail morphologies of (a) and (c).

Figures 2(c) and 2(d) show the cross-sectional SEM images of LISC regions after etching. Grooves were formed from the former regions and when we extended etching time, other regions maintained unetched. The groove was slightly V-shaped, with the width of  $5 - 7 \mu\text{m}$  and the length of  $104.8 \mu\text{m}$ . There existed an irregular layer at the bottom of the groove with about  $15 \mu\text{m}$  long. The aspect ratio (completely etched depth divided by width) was about 16.

#### 3.2 Element analyses

To understand the formation mechanism of grooves, we adopt EDX to analyze the contained element of LISC regions. Figure 3(a) shows the cross-sectional SEM image of one region formed at the laser fluence of  $11.14 \text{ J/cm}^2$ . Figures 3(c) and 3(d) demonstrate the atomic percentage of oxygen in horizontal (x axis) and vertical (z axis) directions in the region before chemical etching. According to EDX measurements, laser irradiation introduced only oxygen into silicon and the oxygen had certain regularities in distribution. The atomic percentage of oxygen in line 3 [Fig. 3(d)] illustrates that oxygen content decreased along the depth (z axis). Horizontally, the oxygen content at the center was much higher than that at the edge of the region, seen from the oxygen analysis of line 1 and 2 in Fig. 3(c).

These results imply that oxygen could be incorporated deep into silicon. Two essential factors may contribute to the oxygen incorporation. One factor is the inducing of dangling bonds in silicon by femtosecond laser irradiation, which made it possible to trap oxygen [21]. The other factor is the local heating effect related to the instantaneous accumulation of laser energy and high absorption, which facilitated the diffusion of oxygen thermally [24]. When femtosecond laser irradiated the silicon, the original regular crystal structures of silicon were

broken and structure changes such as dislocations came into being [25]. Amount of dangling bonds which could trap oxygen appeared in LISC regions. Higher laser fluence and multi-pulse accumulation would deepen the LISC regions and increase the dangling bond density. By thermal activation, oxygen diffused and was trapped by dangling bonds in LISC regions deep into silicon.

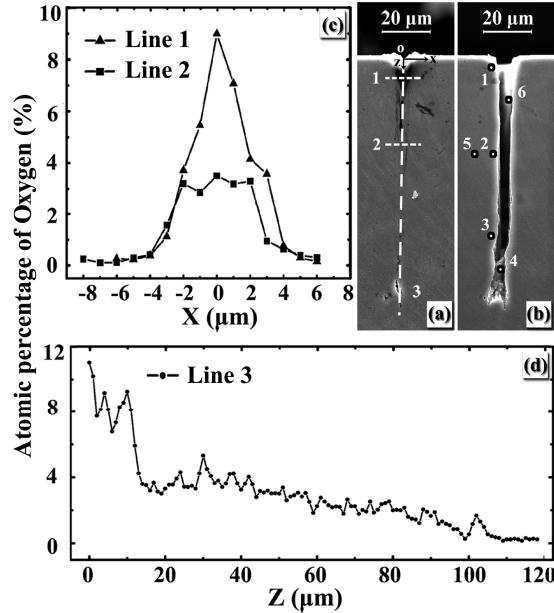


Fig. 3. Element analysis of (a) LISC regions by graph (c) the horizontal orientation line 1 and line 2 and graph (d) the vertical orientation line 3. The vertical axis of two graphs is the atomic percentage of oxygen. (b) showed the EDX analyzing points 1 to 6 of one groove.

EDX analyzing of the groove indicated that materials in oxygenated regions were almost removed after 45 min ultrasonic etching. The chemical composition at the marked positions in Fig. 3(b) was almost pure silicon, therefore the all-silicon grooves were formed.

When it is under non-electrochemical situation at room temperature, HF hardly reacted with silicon without any strong oxidant, so the reaction between silicon and HF could be ignored in our experiments. According to the above results, we could attribute the formation of grooves to the chemical reaction between HF and  $\text{SiO}_x$  formed by femtosecond laser irradiation [26]. To sum up, the HF etching is an oxygen-dependent process. The etching would stop in oxygen-free regions and activate in oxygen-containing regions. The applying of the HF helped to selectively etch the materials in LISC regions to generate grooves. Materials in left regions of the specimen were not etched and remained silicon. The etching rate of the top region was higher than that of the bottom region owing to the higher content of oxygen at the top region. In our experiments the etching time was set long enough to select materials in both top and bottom LISC regions to remove and grooves were observed etching consistently by polishing the sample to a random position.

### 3.3 Influence of laser fluence and scanning velocity on the aspect ratios of grooves

To investigate the influence of laser power on the aspect ratios of grooves, grooves were fabricated at different laser fluences of 1.59, 3.18, 4.77, 6.37, 7.96, 9.55 and 11.14  $\text{J}/\text{cm}^2$  with the scanning velocity of 5  $\mu\text{m}/\text{s}$ . Figure 4(a) shows the aspect ratios of grooves fabricated at these laser fluences. An increase in laser fluence led to an increase in aspect ratio. To research the influence of scanning velocity on the aspect ratios, grooves were fabricated at the scanning velocities of 1, 2, 5, 7, 10, 13, 15  $\mu\text{m}/\text{s}$  with the laser fluence of 11.14  $\text{J}/\text{cm}^2$ . Results indicate

that aspect ratios decreased when scanning velocity increased, seem from Fig. 4(b). In this way, we were able to control the aspect ratio by varying the laser fluence and scanning velocity. In addition, no obvious effect of laser polarization on the aspect ratios was observed in our experiments. Other laser parameters such as focusing position and laser energy distribution profile could also be expected to achieve higher aspect-ratio grooves in silicon.

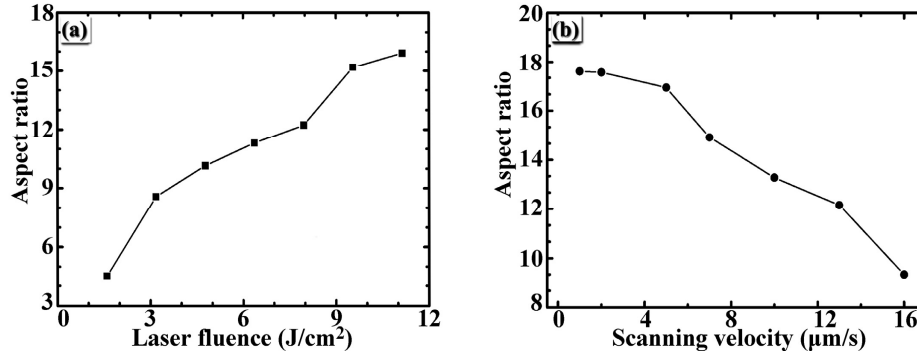


Fig. 4. Dependence of the aspect ratios of grooves on the (a) laser fluence and (b) scanning velocity when the laser beam was focused onto the upper surface of the silicon. For (a) the laser scanning velocity was 5  $\mu\text{m/s}$  and for (b) the fluence is 11.14  $\text{J/cm}^2$ .

#### 4. Conclusion

In conclusion, all-silicon grooves with an aspect ratio of 16 were fabricated by femtosecond laser irradiation combined with oxygen-dependent HF etching. Firstly LISC was induced in silicon by the femtosecond laser irradiation. Secondly HF solution was employed to remove the materials in LISC regions. The formation of grooves could be attributed to the fact that oxygen was incorporated in LISC regions by femtosecond laser irradiation, and materials in oxygenated regions could be etched by HF solution selectively. The aspect ratios of acid-etched grooves increased with the laser fluence and decreased with the scanning velocity. Further, it could be expected that larger-sized grooves or container would be generated by multiple-pass scan. Multi-depth structure can also be fabricated simply at one time by adjusting the conditions of femtosecond laser irradiation process. This method could have potential applications in the fabrication of isolation grooves in MEMS and silicon trench capacitors, as well as micro-fluidic devices of biochemistry.

#### Acknowledgments

The authors gratefully acknowledge the financial support for this work provided by the National Basic Research Program of China (973 Program) under Grant No. 2012CB921804, the National Natural Science Foundation of China (NSFC) under the Grant Nos. 61235003 and 11204236. The authors also sincerely thank Ms. Dai at International Center for Dielectric Research (ICDR) in Xi'an Jiaotong University for the support of SEM and EDS measurements.